Chemistry Journals

Analytical, Inorganic, Organic, Physical, Materials Science

Effect of femtosecond laser pulse repetition rate on nonlinear optical properties of organic liquids

Sandeep Kumar Maurya [1], **Dheerendra Yadav** [1], **Debabrata Goswami** [Corresp. 1]

[1] Department of Chemistry, Indian Institute of Technology, Kanpur, India

Corresponding Author: Debabrata Goswami
Email address: dgoswami@iitk.ac.in

The effect of the repetition rate of femtosecond laser pulses on the two-photon absorption and nonlinear refraction of pure organic liquids is presented using the conventional Z-scan technique. Such a study provides a way to determine the nature of light-matter interaction, explicitly enabling the identification of the linear versus nonlinear regimes. Based on the type of light-matter interaction, we have identified the thermal load dissipation time for the organic liquids. Our experimental results are in good agreement with the theoretically calculated decay time for the dissipation of thermal load.

1   # Effect of Femtosecond Laser Pulse Repetition Rate on
2   # Nonlinear Optical Properties of Organic Liquids
3
4

6   Sandeep K Maurya[1], Dheerendra Yadav[1], Debabrata Goswami[1]
7
8   [1] Department of Chemistry, Indian Institute of Technology, Kanpur, Kanpur 208016, Uttar
9   Pradesh, India
10
11
12
13   Corresponding Author:
14   Debabrata Goswami[1]
15   Department of Chemistry, Indian Institute of Technology, Kanpur, Kanpur 208016, Uttar
16   Pradesh, India
17   Email address: dgoswami@iitk.ac.in

19
20
21
22
23
24
25
26
27
28
29
30
31
32
33
34
35
36
37
38
39
40
41
42

43

Abstract

44 The effect of the repetition rate of femtosecond laser pulses on the two-photon absorption and
45 nonlinear refraction of pure organic liquids is presented using the conventional Z-scan technique.
46 Such a study provides a way to determine the nature of light-matter interaction, explicitly
47 enabling the identification of the linear versus nonlinear regimes. Based on the type of light-
48 matter interaction, we have identified the thermal load dissipation time for the organic liquids.
49 Our experimental results are in good agreement with the theoretically calculated decay time for
50 the dissipation of thermal load.

52

Introduction

54 Over the past few decades, the characterization of Nonlinear Optical (NLO) response of
55 materials has been of great interest to the scientific community due to their potential applications
56 in various fields [1-9]. Pulsed laser sources allow these nonlinear optical processes to occur at
57 low laser power. In light-matter interaction, the transformation of CW laser into pulsed laser
58 gives fascinating space-time control over NLO response. Pulse laser properties (pulse width,
59 wavelength, repetition rate, chirp, and polarization) have shown modulation of a NLO property
60 of materials. Pulse width [10] and wavelength [11,12] have demonstrated a great influence on the
61 nonlinear properties like nonlinear refraction [13], nonlinear absorption [14], and nonlinear
62 scattering [15,16], depending on the properties of the target material. Depending on the
63 molecular property, one can get the order of magnitude difference in the two-photon absorption
64 cross-section (TPACS) by the varying pulse width [17].
65 In the recent past, the effect of polarization [18-20] and repetition rate [21-24] of laser pulses on
66 the nonlinear optical properties of materials have been of great interest to the scientific
67 community. Nonlinear Refraction (NLR) of pure liquids (isotropic media) has not been studied
68 thoroughly as far as the repetition rate of the pulse laser is concerned [20]. However, all
69 materials exhibit focusing and defocusing effects [25] upon interaction with a pulsed laser,
70 which, in turn, depend on the repetition rate of the laser pulses. In the recent past, a vast study on
71 the effect of high repetition rate (HRR) laser pulses have been reported, where thermal load due
72 to a train of laser pulses overwhelm pure single pulse NLO effects. There have been several
73 attempts to obtain the pure NLO property free from thermal inhibition from intense laser pulses.
74 In recent years, optical chopper and pulse picker are being used to manage the cumulative
75 thermal effect in the optical medium [26-30]. However, these techniques have their limitations
76 due to their operating principles. For instance, use of optical chopper in the determination of
77 NLO property minimizes the cumulative thermal effect from intense HRR laser pulses [31,32]
78 with an enhancement in the signal to noise ratio (SNR) for the nonlinear optical effect.
79 Mechanism of focusing and defocusing phenomenon in materials can be understood by the fact
80 that a molecule gets excited upon interaction with light. It may then lose energy by radiative and
81 non-radiative pathways, resulting in thermal load near the illuminated volume. Thermal decay
82 times are in the order of milliseconds or higher. This results in the heating of the material leading

83   to a change in its refractive index (n_2). Depending on the change in the refractive index in the
84   material, there can be a positive refractive index change (convergence of light) known as 'self-
85   focusing' or a negative refractive index change (divergence of light) known as 'self-defocusing'.
86   The Z-scan technique is one of the most straightforward and conventional methods to study the
87   nonlinear optical property of materials, which was proposed by M. Sheik-Bahae and E.W. Van
88   Stryland [33] for the determination of nonlinear refraction index. They have shown the reversal
89   of sign in the nonlinear index of refraction with the variation of wavelength [34]. The Z-scan
90   technique can determine the two-photon absorption cross-section (σ_2) and nonlinear index of
91   refraction (n_2), which are directly related to the imaginary and real part of the third order
92   nonlinear susceptibility, respectively. In general, the determination of NLO properties is
93   performed in a conventional and readily available solvent (like Methanol, dichloromethane,
94   dimethyl sulfoxide, etc.), which must be fully transparent to the laser frequency. However, these
95   solvents also go to the non-resonant thermal heating with ultrashort laser pulses. The primary
96   aim of this paper is to address the associated thermal effect with the interaction of femtosecond
97   laser pulses to organic liquids. Choice of our organic liquids solemnly depends on the nonlinear
98   absorption characteristic to study the influence of thermal load on nonlinear refraction and
99   nonlinear absorption.
100   Herein, we report the effect of repetition rate on the nonlinear optical property of methanol
101   (CH_3OH) and carbon disulfide (CS_2) as an organic solvent. Organic liquids were chosen based
102   on their nonlinear optical properties around the central wavelength of the laser. While CH_3OH
103   exhibits only nonlinear refraction, CS_2 exhibits both two-photon absorption and nonlinear
104   refraction upon interaction with a femtosecond laser pulse at 800 nm. This study was aimed to
105   investigate the influence of repetition rate on nonlinear refraction and to determine the thermal
106   decay time (τ) for both the organic liquids.
107
Materials & Methods
108
109   Our femtosecond experimental setup involves a tunable repetition rate Ti:Sapphire Regenerative
110   Amplifier System (Spitfire-Pro, Spectra-Physics Inc. USA) that is seeded with a Spectra-Physics
111   Mai-Tai Ti:Sapphire oscillator, having 82 MHz repetition rate with wavelength tunability of
112   780–820 nm. The maximum repetition rate experiments were performed with the broadband
113   Mai-Tai oscillator at 82 MHz. The amplifier cavity with two Pockel's cells makes the different
114   repetition rates possible as an interplay of the time of injection of the seed pulse in the amplifier
115   cavity and the dump time that extracts the amplified pulse out of the cavity. Consequently, we
116   were able to generate amplified laser pulses of different repetition rates, such as 5, 10, 20, 25, 50,
117   100, 200, 250, 333, 500, and 1000 Hz. Figure 1 shows a schematic of the experimental setup,
118   which describes closed aperture Z-scan (CAZS) and open aperture Z-scan (OAZS) schemes.
119   Femtosecond pulses from the amplifier were focused using a 20 cm lens onto a 1 mm quartz
120   cuvette. The cuvette contains a liquid sample for Z-scan experiments, where the path length of
121   the sample cell satisfies the condition that the cell-length is less than the Rayleigh range of the
122   focusing lens. Rayleigh range in our setup was 1.3 mm at 800 nm, as the beam waist at the focal

123 point was 18 μm. We scanned the sample through the focal point of the lens using a motorized
124 translation stage (Newport Inc. model ESP 300), whose minimum step size is 0.1 μm. This
125 allows for a smooth intensity scan of the sample. To ensure the least interference from material
126 dispersion from femtosecond pulses, all the mirrors used in our setup were zero-dispersion
127 mirrors under our experimental conditions.
128 The transmitted beam through the sample is focused with a lens of 10 cm focal length into a UV-
129 enhanced PDA100A-EC - Si Switchable Gain Detector. The peak-to-peak values from the
130 photodiode are measured with an LTM-354 LeCroy oscilloscope, which is triggered by laser
131 frequency for each repetition rate. The reference signal from detector D_1 was also recorded for
132 the normalization of the signal from detectors D_2 and D_3. The delay stage and the oscilloscope
133 are interfaced with the computer using a GPIB card (National Instruments Inc.), and the data is
134 acquired using LabVIEW programming. After acquiring the data, results were fitted in the
135 following equation, for the open aperture z scan data [32]:

136
$$T(z) = 1 - \frac{\beta I_0 L}{2\sqrt{2}\left(1 + \frac{z^2}{z_0^2}\right)} \qquad\qquad (1)$$

137 where β, I_0, L and z is the two-photon absorption coefficient, the intensity of femtosecond laser
138 pulse at the focus in Jcm^{-2}, sample thichness and sample position respectively. At different z
139 positions, transmittance T is calculated, and since all the other parameters are known, β can be
140 calculated easily. Subsequent to obtaining the values of β, the TPA cross-section of
141 chromophore (σ_2, in units of GM, where $1\ GM = \frac{10^{-50} cm^4 . s}{photon.molecule}$) is generated from the expression:
142 $\sigma_2 = \beta h\nu^* 10^3/Nc$, where ν is the frequency of the incident laser beam, N is Avogadro constant,
143 c is the concentration of the molecule in respective solvents, while equation 2 was used to fit the
144 close aperture z-scan data [32, 33]:

145
$$T(z,\Delta\varphi_0) = 1 + \Delta\varphi_0 \frac{4x}{(x^2 + 1)(x^2 + 9)} \qquad\qquad (2)$$

146 where, x = z/z$_0$, Δφ$_0$(t) = kΔn$_0$(t)L, and k = 2π/λ is known as wave vector. Λ denotes the
147 wavelength and Δn$_0$(t) = n$_2$I$_0$(t), where, n$_2$ is the coefficient of nonlinear refraction in the unit of
148 m^2/W.
149

Results and Discussion

151 The Z-scan experiment for the organic liquids, CS_2 and CH_3OH, was carried out at 800 nm, for
152 which, both the liquids were transparent at low laser pulse power. However, at high powers of
153 the femtosecond laser pulse, CS_2 exhibits two-photon absorption (TPA). Both open aperture and
154 close aperture Z-scan techniques were used for studying the influence of repetition rate on
155 nonlinear refraction (NLR) and Two-photon absorption cross-section (TPACS) of the organic

156 solvent. To achieve the desired nonlinear response from these liquids, we have used average
157 laser power of 145 GW/cm^2 where methanol exhibit only NLR and CS$_2$ exhibit both NLR and
158 TPA. OAZS trace of CS$_2$ is shown in Fig. 2(a), while the CAZS traces for both the organic
159 liquids are shown in Fig. 2(b) at 1 kHz repetition rate. These organic liquids exhibit a positive
160 nonlinear index of refraction (valley-peak) at 1 kHz, as compared to a negative nonlinear index
161 of refraction (peak-valley) at 82 MHz repetition rate of the laser pulse, as shown in Fig. 3. The
162 reversal of sign in the n$_2$ arises from the cumulative thermal load of the train of femtosecond
163 laser pulses with very short pulse-to-pulse intervals [35]. Thermal load generates a diverging lens
164 due to thermal expansion (hence negative n$_2$) and since both methanol and carbon disulfide have
165 negligible absorption at 800 nm, their n$_2$ values are similar.
166 The impact of thermal load can be further understood from the concept of acoustic transit time
167 (τ_{ac}), which is a ratio of beam waist at the focus and, the speed of sound in the medium [36].
168 Beam waist of our Z-scan setup at the focus was found to be 18 μm, and the speed of sound
169 happened to be 1103 m/s and 1149 m/s for methanol [37] and carbon disulfide [38]. Hence, the
170 calculated τ_{ac} for the respective liquids are 16.3 ns and 15.7 ns. This indicates that pulse-to-pulse
171 separation in MHz regime is in comparison with acoustic transit time, whereas in kHz regime,
172 the separation between two consecutive pulses is in the orders of a couple of magnitudes longer
173 than acoustic transit time in both the organic liquids. Hence, the thermal load is expected to
174 occur in organic liquids with MHz repetition rate laser, which in turn, results in the thermal lens
175 effect in these liquids. This eventually leads to the negative nonlinear index of refraction in
176 MHz, whereas the positive nonlinear index of refraction was observed in 1 kHz laser pulses.
177 Apart from the acoustic transit time of these organic liquids, thermal conduction time also plays
178 an important role in the negative index of nonlinear refraction, which is given by the following
179 equations [39,40]:

180 $\tau = \dfrac{\omega_0^2}{4K}$ (3)

181 $K = \dfrac{\kappa}{\rho c_p}$ (4)

182 where K is the thermal diffusivity, ω_0 is the beam waist at the focus of the lens, ρ is the density
183 of the liquid, c_p is specific heat capacity and κ is the thermal conductivity of the liquid. Given the
184 above mentioned parameters for methanol: $\rho = 0.791\ gcm^{-3}$, $c_p = 2.56\ Jg^{-1}K^{-1}$, $k = 0.203\ W$
185 $m^{-1}K^{-1}$, and for carbon disulfide (CS$_2$): $\rho = 1.263\ gcm^{-3}$, $c_p = 0.995\ Jg^{-1}K^{-1}$, $k = 0.16\ W$
186 $m^{-1}K^{-1}$, and $\omega_0 = 18\ \mu m$, the calculated thermal conduction time under our experimental
187 condition is 0.82 ms for methanol and 0.64 ms for CS$_2$. Thus, the thermal lens is apparent in
188 these liquids at a high repetition rate of the laser pulses, resulting in a self-defocusing effect with
189 negative n_2 in these liquids. On the other hand, at 1 kHz, the system exhibits a self-focusing
190 effect with positive n_2. The calculated value of the n$_2$ with the fitting of the CAZS trace is 1.2 ×

191    $10^{-7} cm^2/GW$ for methanol, and $2.7 \times 10^{-6} cm^2/GW$ for CS_2 at 800 nm, for 45 fs pulse at 1

192   kHz repetition rate. TPA coefficient for CS_2 was found to be: $4 \times 10^{-2} cm/GW$. These results

193   are in good agreement with the values found in the literature [41-43].

194   Laser power was adjusted in such a way that there was no distortion in the pulse profile of the

195   laser while propagating through the medium. Under the same experimental condition, by keeping

196   the constant intensity of laser pulses, CAZS experiment was carried out for both liquid samples

197   at each repetition rate varying from 1 kHz to 10Hz. CAZS trace at variable repetition rate is

198   shown in Fig. 4 for the methanol, whereas OAZS trace for CS_2 is shown in Fig. 5. CAZS study

199   with varying repetition rate show a measurable change in the peak-valley transmittance in both

200   the liquids, which eventually resulted in the nonlinear index of refraction as presented in Fig.

201   6(a) and 6(b) for methanol and CS_2, respectively. The change in n_2 was observed with the

202   variation of the repetition rate of the laser pulses. Modulation in the nonlinear index of refraction

203   with the variation of the repetition rate of the laser is a consequence of thermal load on the

204   liquids due to the single laser pulse interaction, which generally decay in milliseconds to second

205   timescales depending on the thermo-optical property of the liquids. Typically, the mechanism of

206   the thermal decay consists of conduction, convection and radiative processes. Out of these

207   possibilities, thermal decay by convection varies from situation to situation irrespective of

208   materials and is hard to predict. As mentioned earlier, probable contribution to the change in n_2

209   could due to the influence of thermal conductivity. Our study on the nonlinear index of refraction

210   with a variable repetition rate provides some opportunity to implement the pulse-to-pulse

211   separation of the laser to determine the thermal decay in liquids. As shown in Fig. 6, we have

212   implemented the pulse-to-pulse separation ranging from 1 ms to 0.1 s, which has a direct

213   influence on the nonlinear index of refraction. The variations obtained in the nonlinear index of

214   refraction have been fitted with a double exponential model, which resulted in the two-time

215   constants T_1 and T_2. The time constant T_1 can be accounted for thermal decay time, which

216   represents the time required for the complete removal of thermal effect due to femtosecond laser

217   pulses. On the other hand, time constant T_2 somewhat associated with the effect of broadening of

218   pulses (as shown in Fig. 7, which was measured using noncollinear autocorrelation technique

219   alongside the measurement of z-scan) along with the effect of convection and other non-radiative

220   time decays. Since, heat accumulation on transparent liquid due to intense laser pulses can decay

221   through heat conduction and convection [44] whose time scale can be orders of magnitude

222   different depending on the resonant (highly absorbing liquid) and nonresonant (non-absorbing

223   liquid) thermal accumulation [45]. The time constant associated with T_2 were further analyzed

224   and attributed to the broadening of the pulse due to the support of the TPACS variation as a

225   function of the pulse to pulse separation (Fig. 8), which were found to be same as the time

226   constant obtained from the variation of NLR. As shown in Fig. 8, it is not possible to discern the

227   trend even on including all possible causes of errors that may creep in the calculation of the

228   TPACS. It is observed from the CAZS experiments that the thermal load is apparent even at a

229   low repetition rate of the laser pulse, such as, 1 kHz, which further diminishes, as the pulse-to-

230   pulse separation increases with the decrease of repetition rate. A pictorial representation of this

231 variation is shown in Fig. 9. Thus, for the first time, we report here, the thermal decay time
232 constant probed by the conventional z scan technique as a variation of pulse repetition rate,
233 which was found to be on the order of the calculated thermal conduction time as tabulated in
234 Table 1.
235

Conclusions

237 Here, we have presented the study of the effect of repetition rate on the nonlinear index of
238 refraction of methanol (CH_3OH) and carbon disulfide (CS_2), using femtosecond laser pulses at
239 800 nm. This study indicates that the nonlinear index of refraction is prone to the pulse-to-pulse
240 separation as compared to the nonlinear absorption, which does not show any significant change
241 with respect to the repetition rate of the laser. This result also exhibits that working with laser
242 pulses as low as 100 Hz or lower [46] can give rise to almost pure nonlinear optical properties.
243 Experimentally calculated thermal decay time from this study was found to be in good agreement
244 with the theoretically calculated thermal conduction time for both the organic liquids under
245 consideration.
246

Acknowledgments

248 All the authors acknowledge Ms. S. Goswami for extensive language editing of this article.
249
250
251
252

References

254 1. C. N. LaFratta, J. T. Fourkas, T. Baldacchini, R. A. Farrer, *Angew. Chem. Int. Ed*. 2007,
255 **46**, 6238-6258.

256 2. C. N. LaFratta, J. T. Fourkas, T. Baldacchini, R. A. Farrer, *Angew. Chem*. 2007, **119**,
257 6352-6374.

258 3. C. W. Spangler, *J. Mater. Chem*. 1999, **9**, 2013-2020.

259 4. W. G. Fisher, W. P. Partridge, Jr., C. Dees, E. A. Wachter, *Photochem. Photobiol*. 1997,
260 **66**, 141-155.

261 5. W. R. Zipfel, R. M. Williams, W.W. Webb, *Nat. Biotechnol*, 2003, **21**, 1369-1377.

262 6. F. Helmchen, W. Denk, *Nat. Methods*, 2005, **2**, 932-940.

263 7. D. A. Parthenopoulos, P. M. Rentzepis, *Science*, 1989, **245**, 843-845.

264 8. S. Kawata, Y. Kawata, *Chem. Rev.* 2000, **100**, 1777-1788.

265 9. T.-C. Lin, S.-J. Chung, K. S. Kim, X. Wang, G. S. He, J. Swiatkiewicz, H. E. Pudavar, P.
266 N. Prasad, *Adv. Polym. Sci*. 2003, **161**, 157-193.

267 10. J. Yi, M.-G. Baik, J. Han, H. Park, Y. Rhee, J. Lee, *J. K. Phys. Soc*. 1998, **33**, 297-300.

268 11. N. K. M. N. Srinivas, S. V. Rao, V. G. L. N. Rao, B. K. Kimball, M. Nakashima, B. S.
269   Decristofano, D. N. Rao, *J. Porphyrins Phthalocyanines*, 2001, **5**, 549-554.

270 12. J. Szeremeta, R. Kolkowski, M. Nyk, M. Samoc, *J. Phys. Chem. C*, 2013, **117**, 26197-
271   26203.

272 13. A. Major, F. Yoshino, I. Nikolakakos, J. S. Aitchison, P. W. E. Smith, *Opt. Lett*. 2004,
273   **29**, 602-604.

274 14. A. N. Golubev, S. I. Nikitin, M. A. Smirnov, A. L. Stepanov, *J. Phys.: Conf. Series*,
275   2011, **324**, 012038.

276 15. K. Clay, K. Wostyn, A. Persoons, *Adv. Funct. Mater*. 2002, **12**, 557-563.

277 16. S. J. Matcher, M. Cope, and D. T. Delpy, *Adv. Opt*. 1997, **36**, 386-396.

278 17. C. Xu, W. W. Webb, *J. Opt. Soc. Am.* B 1996, **13**, 481-491.

279 18. M. G. Vivas, L. De Boni, Y. Bretonniere, C. Andraud, C. R. Mendonca, *Opt. Exp*. 2012,
280   **20**, 18600-18608.

281 19. L. Chen-Hui, Z. Hui, Z. Shi-An, S. Zhen-Rong, *Chin. Phys. B*, 2012, **21**, 123202.

282 20. J. O' Dowd, W. H. Guo, E. Flood, M. Lynch, A. L. Bradley, L. P. Barry, J. F. Donegan,
283   *Opt. Exp.* 2008, **16**, 17682-17688.

284 21. M. Yuksek, T. Ceyhan, F. Bagci, H. G. Yaglioglu, A. Elmali, O. Bekaroglu, *Opt. Comm*.,
285   2008, **281**, 3897–3901.

286 22. C. Gorling, U. Leinhos, K. Mann, *Opt. Comm*. 2003, **216**, 369–378.

287 23. L. Yin, G. P. Agrawal, *Opt. Lett*. 2007, **32**, 2031-2033,

288 24. W. Liu, B. Li, *Chinese Optic Lett*. 2013, **11**, 053002(1-3).

289 25. M. Sheik-Bahae, A. A. Said, D. J. Hagan, M. J. Soileau, E. W. Van Stryland, *Opt. Eng.*
290   1991, **30**, 1228-1235.

291 26. A. Gnoli, L. Razzari, M. Righini, *Opt. Exp*. 2005, **13**, 7976-7981.

292 27. A Nag, A. K. De, D. Goswami, *J. Phys.: Conf. Ser*. 2007, **80**, 012034,

293 28. J. A. Davila Pintle, E. R. Lara, M. D. Iturbe Castillo, *Opt. Exp*. 2013, **21**, 15350-15363.

294 29. R. Edziah, E. Lalanne, V. Torres, A. M. Johnson, S. Trivedi, *J. Opt. Soc. Am. B*, 2011,
295   **28**, 1385-1390.

296 30. A. Shehata and T. Mohamed, *J. Opt. Soc. Am. B*, 2019, **36**(5), 1246-1251.

297 31. A. Shehata, M. Ali, R. Schuch, T. Mohamed, *Optics & Laser Technology*, **116**: 276-283.

298   32.   A. Nag, A. K. De, D. Goswami, *J. Phys. B: At. Mol. Opt. Phys*. 2009, **42**, 065103(1-7).

299   33.   M. Sheik-Bahae, A. A. Said, E. W. Van Stryland, *Opt. Lett.* 1989,**14**, 955-957.

300   34.   M. Sheik-Bahae, A. A. Said, T.H. Wei, D. J. Hagan, E. W. Van Stryland, *J. Quant.*

301   *Electr*. 1990, **26**, 760-769.

302   35.   R. L. Harzic, N. Huot, E. Audouard, C. Jonin, P. Laporte, S. Valette, A. Fraczkiewicz, R.

303   Fortunier, *Appl. Phys. Lett*. 2002, **80**, 3886-3888.

304   36.   D. I. Kovsh, D. J. Hagan, E. W. Van Stryland, *Opt. Exp*. 1999, **4**, 315-327.

305   37.   M. J. Dávila, J. P. M. Trusler, *J. Chem. Thermodynamics*, 2009, **41**, 35–45.

306   38.   K. F. Herzfeld, T. A. Litovitz, *Absorption and Dispersion of Ultrasonic Waves*

307   (Academic Press, New York, 1959).

308   39.   M. Falconieri, G. Salvetti, *Appl. Phys. B* 1999, **69**, 133-136.

309   40.   J. P. Gordon, R. C. C. Leite, R. S. Moore, S. P. S. Porto, J. R. Whinnery, *J. Appl. Phys*.

310   1965, **36**, 3-8.

311   41.   S. Couris, M. Renard, O. Faucher, B. Lavorel, R. Chaux, E. Koudoumas, X. Michaut,

312   *Chem. Phys. Lett*. 2003, **369**, 318-324.

313   42.   R. A. Ganeev, A.I. Ryasnyansky, N. Ishizawa, M. Baba, M. Suzuki, M. Turu, S.

314   Sakakibara, H. Kuroda, Opt. *Comm*. 2004, **231**, 431-436.

315   43.   J. W. Wilson, P. Samineni, W. S. Warren, M. C. Fischer, *Bio. Opt. Exp*. 2012, **3**, 854-

316   862.

317   44.   P. Kumar, A. Khan, D. Goswami, Chem. Phys. 2014, **441**, 5-10.

318   45.   P. Kumar, S. Dinda, D. Goswami, Chem. Phys. Lett. 2014, **601**, 163-167.

319   46.   S. Singhal, S. Dinda, D. Goswami, *Appl. Opt.* 2017, **56**, 644-648.

Figure 1

Experimental Setup.

Schematic of the experimental setup for open aperture and close aperture z-scan technique. While the amplified laser output at various repetition rate was used directly, the laser oscillator output for the experiment was additionally chirp-compensated with a prism pair.

 Chemistry Journals
Analytical, Inorganic, Organic, Physical, Materials Science
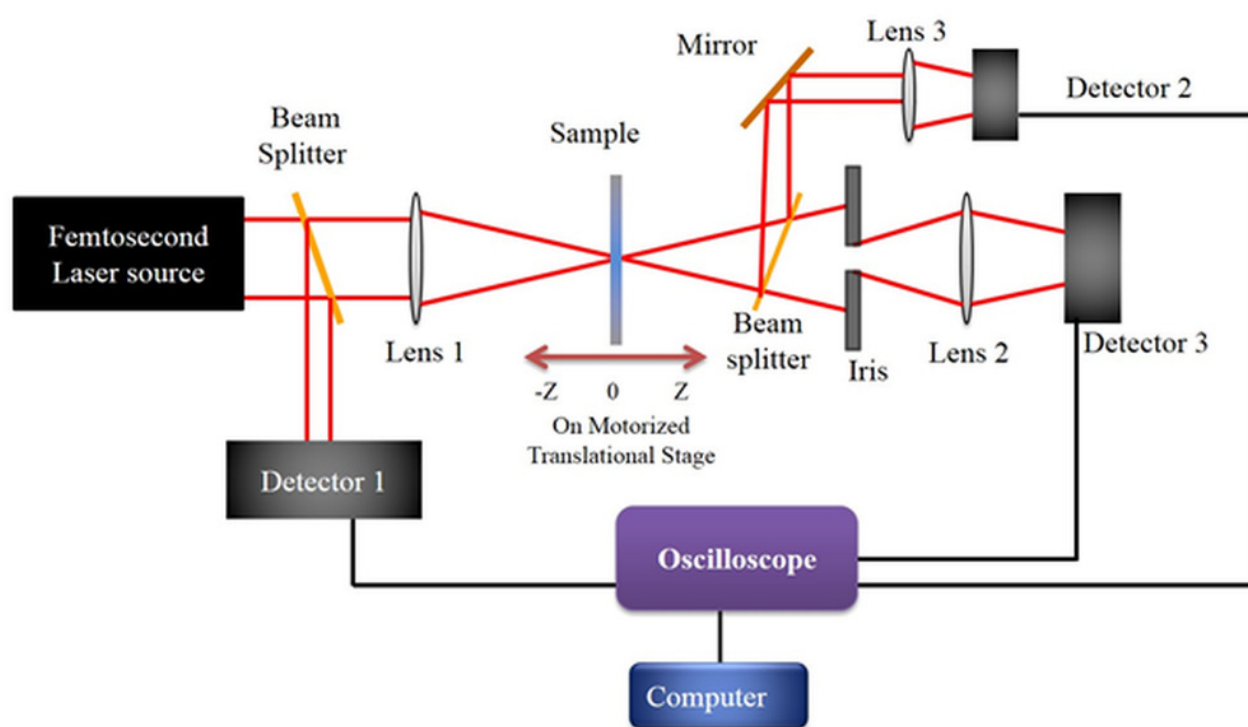
Figure 2

Open and close aperture z-scan.

(a) Open aperture z-scan trace and (b) Close aperture z-scan trace of Methanol and Carbon disulfide at the power of 145 GW/cm^2 using 45 fs pulse width laser pulse at 800 nm.
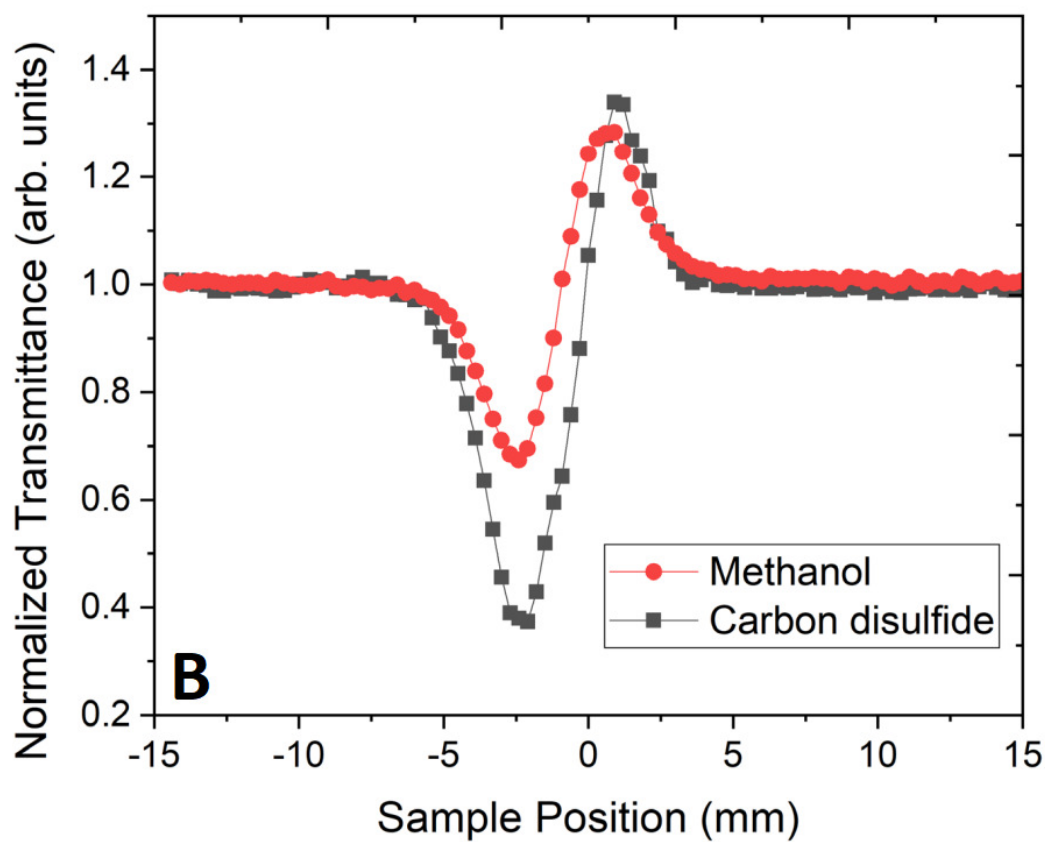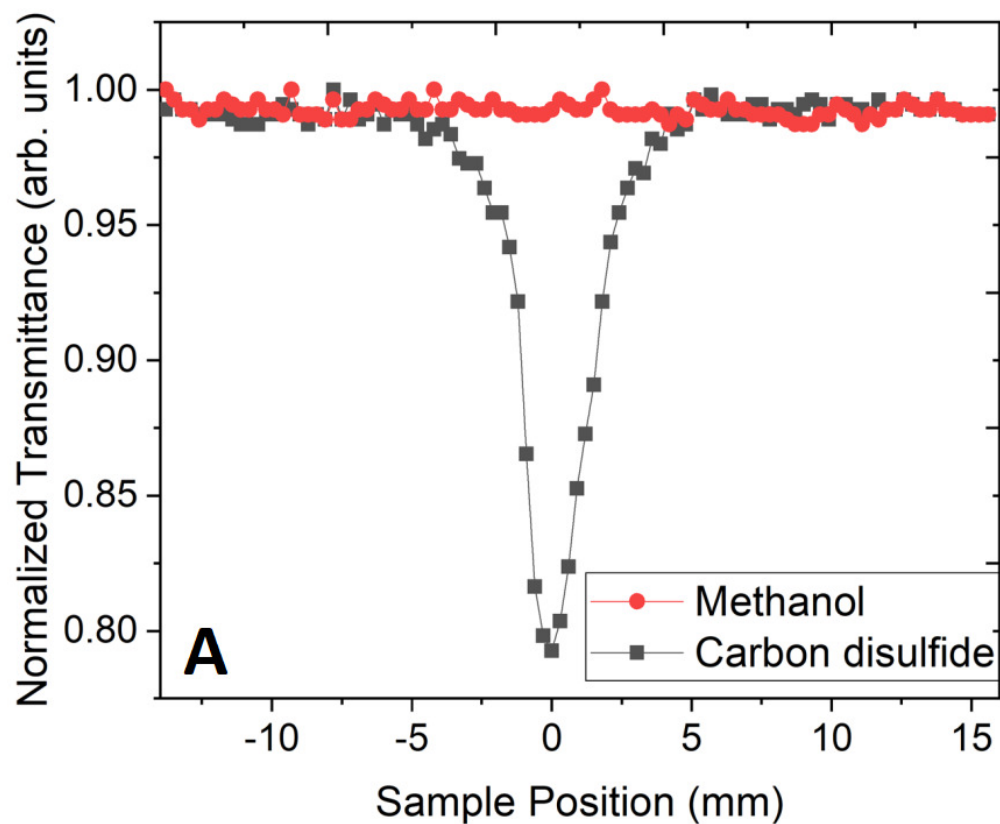
Figure 3

Close aperture z-scan trace at high repetition rate laser.

Close aperture z-scan trace of CH_3OH and CS_2 at 800 nm with 40 fs chirp-compensated laser pulses from the laser oscillator with an average power of 11 GW/cm^2 at the focus of 20 cm lens having a repetition rate of 82 MHz.
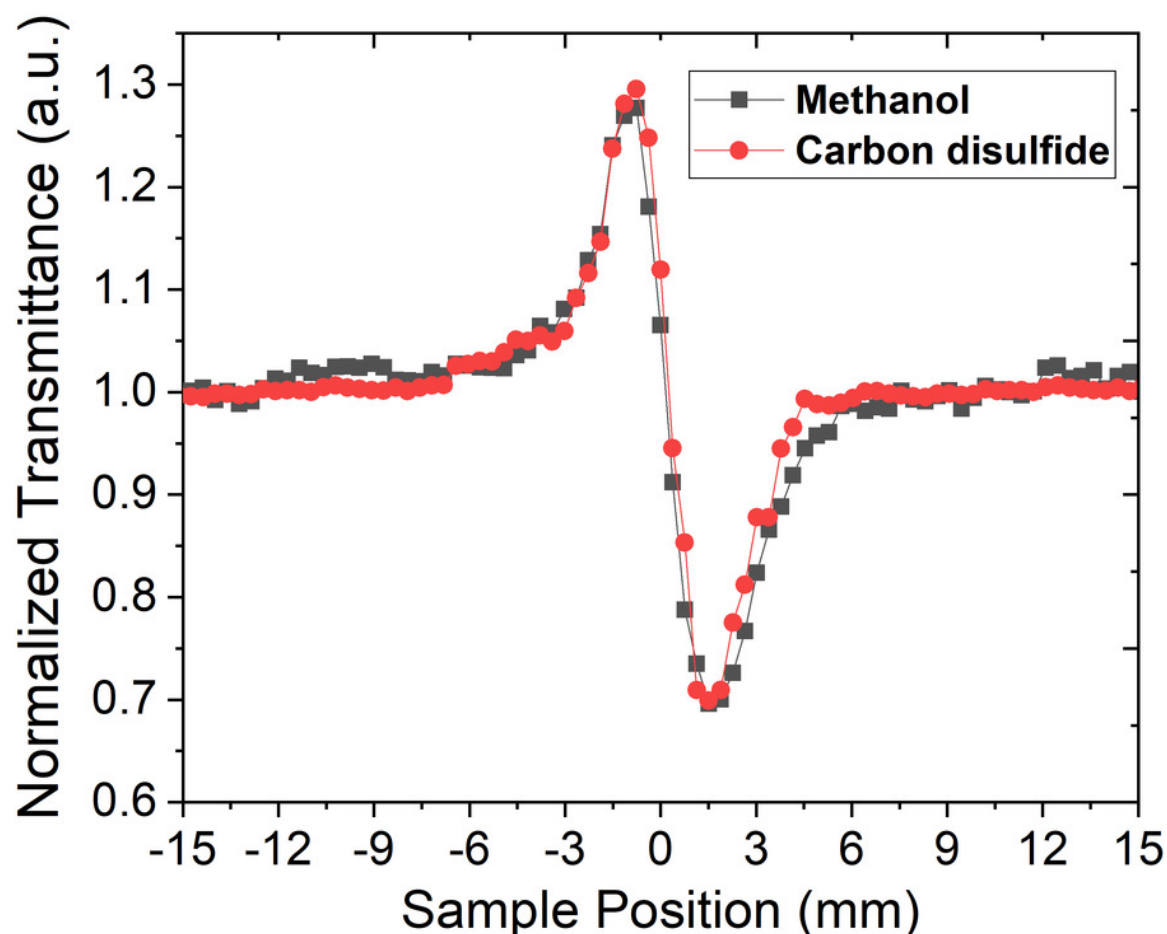
Figure 4

Close aperture z-scan trace at different laser repetition rates.

Close aperture z-scan trace of methanol at 800 nm from an amplifier at different repetition rate having laser pulses ranging from 45 to 110 fs, where average power of the laser pulse was kept constant.
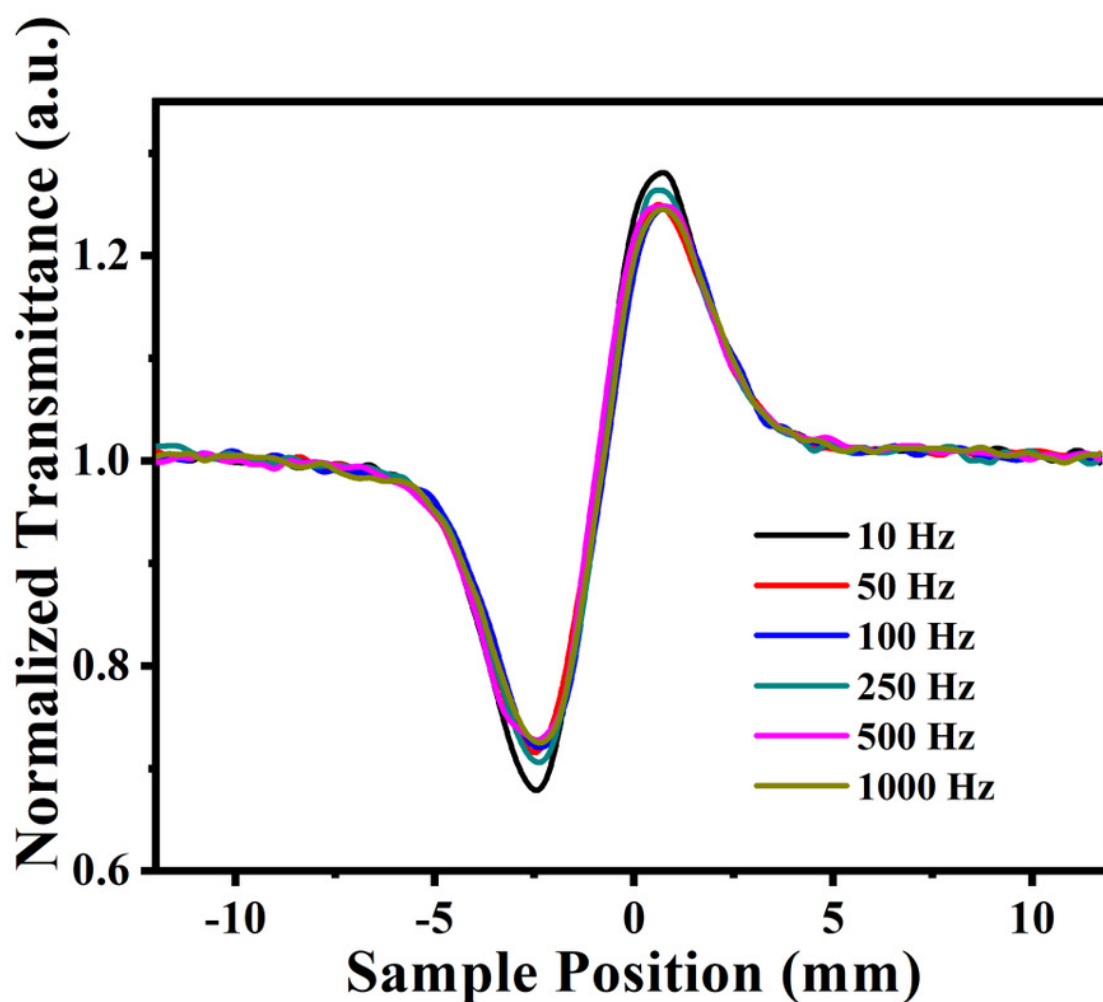
Figure 5

Open aperture z-scan trace at different repetition rates.

Open aperture z-scan trace for carbon disulfide at 800 nm with 45 fs pulse width and average

power of 145 GW/cm^2 for carbon disulfide at 1 kHz from Ti:Sapphire regenerative amplifier.
Note that methanol does not show any open aperture z-scan, as shown in Fig. 4.
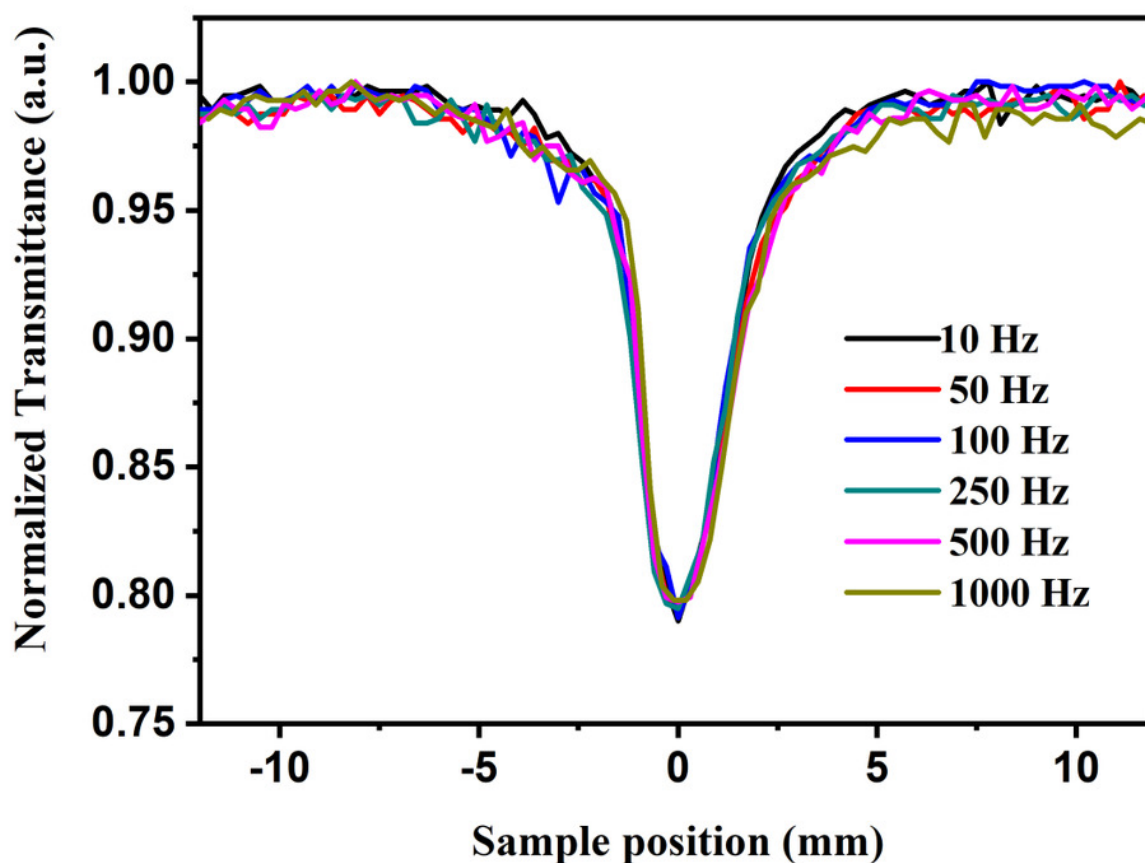
Figure 6

Variation of nonlinear index of refraction with pulse to pulse seperation.

Variation of nonlinear index of refraction as a function of the pulse to pulse separation for femtosecond laser pulses (ranging from 45 to 110 fs) for (a) methanol (CH_3OH) and (b) carbon disulfide (CS_2) in close aperture z-scan.
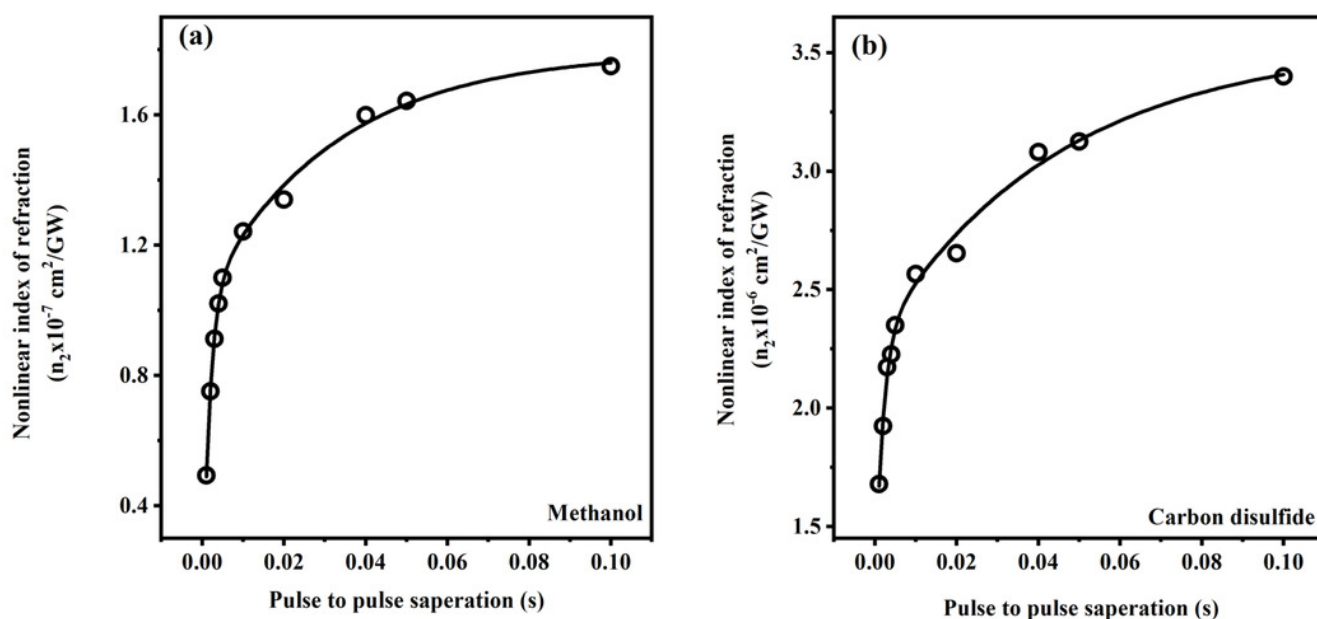
Figure 7

Variation of measured pulse width at different repetition rates.

(a) Pulse width measurements (45 to 110 fs) at a different repetition rate of the laser amplifier at 800nm, and (b) Variation of the pulse width with the laser repetition rate.
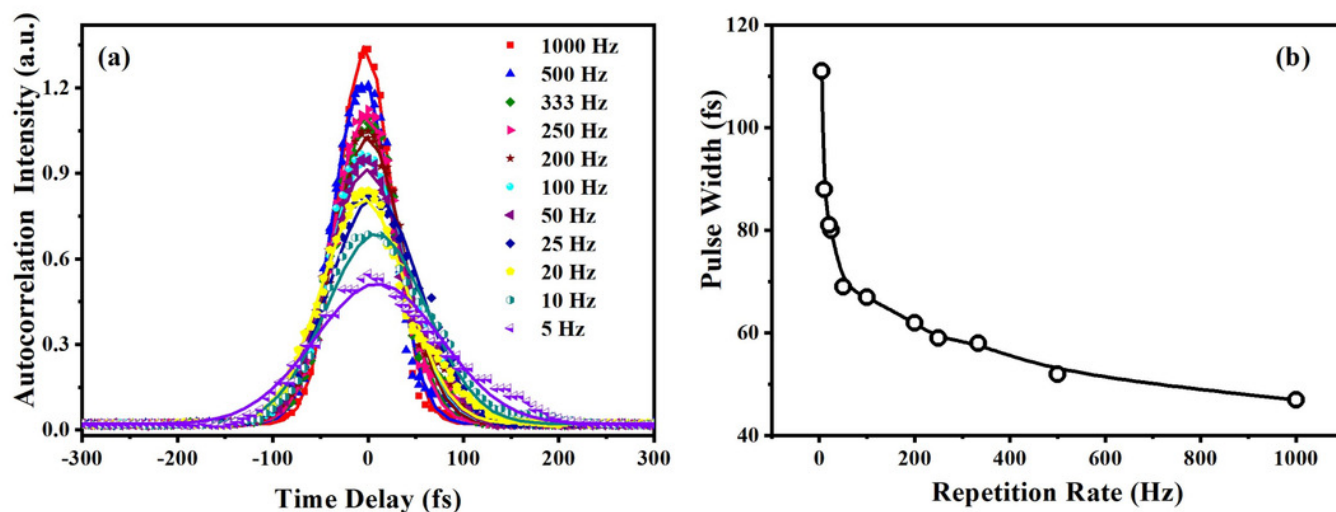
Figure 8

Variation of TPACS with pulse to pulse separation.

Variation of TPA cross-section as a function of the pulse to pulse separation of the laser pulses (ranging from 45 to 110 fs) at 800 nm for carbon disulfide (CS_2) in open aperture z-scan.
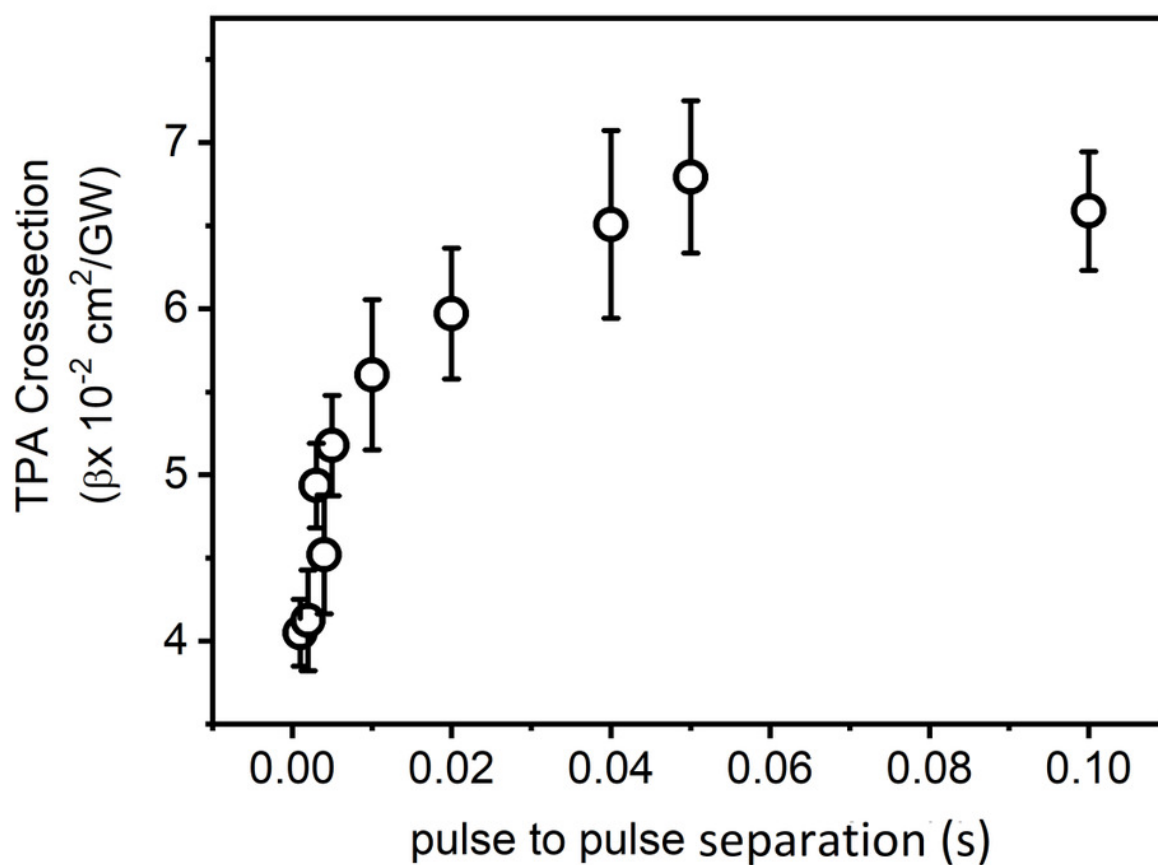
Figure 9

Cartoon of close aperture z-scan traces as a function of the variation of pulse-to-pulse separation.

Schematic profile of close aperture z-scan traces as a function of the variation of pulse-to-pulse separation where x-axis represents the sample position and the y-axis represents the normalized transmittance.
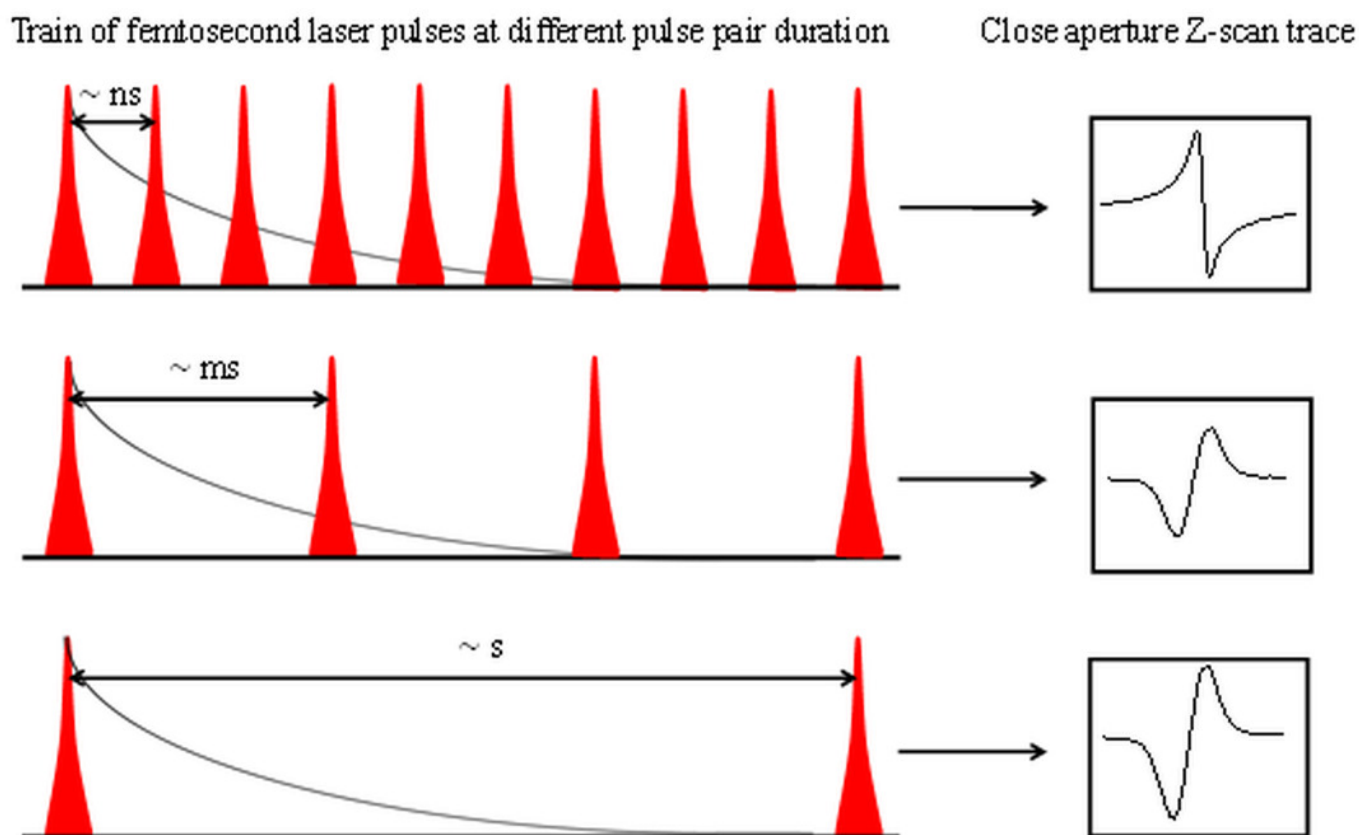
Chemistry Journals

Analytical, Inorganic, Organic, Physical, Materials Science

The thermal decay time constant as a variation of pulse repetition rate.

A double exponential fit of the change in transmittance with respect to pulse pair separation provides the calculated thermal conduction time. The thermal decay time constant as a variation of pulse repetition rate is of the same order as the calculated thermal conduction time.

Double exponential decay fit	$Y = Y_0 + A_1\exp\left(-\dfrac{t}{T_1}\right) + A_2\exp\left(-\dfrac{t}{T_2}\right)$		Theoretically calculated time constant from equation 3
	T_1 (ms)	T_2 (ms)	T_1 (ms)
Methanol	1.74 ± 0.3	32.1 ± 4.4	0.82
Carbon disulfide	1.92 ± 0.5	44.8 ± 1.2	0.64